Journal of Luminescence 195 (2018) 396–401

Contents lists available at ScienceDirect

Journal of Luminescence

journal homepage: www.elsevier.com/locate/jlumin

Luminescence and light guiding properties of Er and Li codoped ZnO nanostructures

F. Pavón, A. Urbieta*, P. Fernández

Departamento de Física de Materiales, Facultad de Ciencias. Físicas, Universidad Complutense de Madrid, Ciudad Universitaria s/n, 28040 Madrid, Spain

ARTICLE INFO

Keywords:
ZnO
Cathodoluminescence
Rare earth doping
Optical properties

ABSTRACT

Micro- and nanostructures of ZnO co-doped with Er and Li ions have been grown by a catalyst free vapor-solid method under constant N_2 flux. Nanowires and nanobelts with lengths of several microns, and thicknesses of a few hundreds of nanometers have been obtained. Scanning Electron Microscopy (SEM), X Ray Microanalysis (EDS) and micro-Raman spectroscopy have been used to characterize the samples. Luminescent emission has been studied by cathodoluminescence (CL). Modifications in the defect structure due to Li incorporation are observed. An increase in the relative intensity of the Er^{3+} - related 0.8 eV (1.54 μm) emission band in the co-doped samples has been observed. Micro-photoluminescence (μ-PL) has been used to investigate the optical properties of the structures. The establishment of optical resonant modes and wave guiding along both the longitudinal and transversal axes of the structures have been observed.

1. Introduction

The unique properties of ZnO have made this material the object of extensive investigation. It is a wide band gap semiconductor with a huge binding exciton energy, and hence an excellent candidate for optoelectronic applications such as blue LED and lasers. Besides the near band edge emissions, intense luminescence in green, yellow and orange-red is also observed. The possibility to tailor the luminescence over this wide range in the visible region has been one of the hottest points in the recent studies on this material [1–3]. Upconversion luminescence in ZnO doped with rare earth ions has been also explored for a variety of applications as infrared detection, fluorescent labels or optical data storage among others [4–7].

Er doping has a particular interest due to the emissions in the infrared region since the 1.54 μm emission has special importance in optical communications applications [8–10]. It is associated to intra-4f transitions ($^4I_{13/2} \rightarrow {}^4I_{15/2}$) via an energy transfer mechanism from excited host electrons to the Er ion [8]. Although the energy transfer mechanism is effective in RE doped semiconductors, the solubility of Er in ZnO lowers the Er related luminescence [11,12]. Two main approaches may be chosen for overcoming this low emission efficiency: fabrication of low dimensional structures (mainly nanorods or nanowires) or codoping to enhance the luminescence efficiency itself. Nanostructuring yields a higher surface area, then increasing the Er solubility and consequently the number of active centers for luminescence. By codoping we distort the close environment of the RE ion, and hence the transition probabilities of the different intra-4f-shell transitions are modified [13,14].

In this work, a synergetic approach has been tackled. We have grown Er-Li co-doped ZnO nanostructures with different morphologies, from nanowires to nanobelts. The influence of lithium content on both morphology and luminescence has been studied. Besides the effect of Li in the visible deep level band, the maximum enhancement of the 1.54 μm band, seem to occur for an intermediate Li content, in agreement with previous works [10].

2. Experimental method

The codoped micro- and nanostructures were obtained by Vapor-Solid method (VS) from a mixture of powders of ZnS, Er_2O_3 and Li_2O (99.999%, 99.9% and 99.5% purity, respectively) in different proportions. The weight percentage Er_2O_3 was set at 5 wt% for all samples (1.09 at% when only Er is present), since, in previous works, it has been determined to be an optimum value [15,16]. Li_2O content is varied from 1 to 10 wt%. A reference sample with no lithium has been also studied. Table 1 summarizes the compositions of the samples used in this work

In all cases, the mixtures were homogenized by ball milling in a centrifugal ball mill with 20 mm agate balls for 5 h at 180 rpm. The final powder was compacted under a 1 T compressive load to form disk shaped samples of about 7 mm diameter and 2 mm thickness. The samples were then placed on an alumina boat and annealed in a

* Corresponding author.
E-mail address: anaur@ucm.es (A. Urbieta).

https://doi.org/10.1016/j.jlumin.2017.11.059
Received 27 August 2017; Received in revised form 28 November 2017; Accepted 30 November 2017
Available online 01 December 2017

Table 1
Summary of sample compositions.

Weight %	Er atomic %	Li atomic %
ZnO: 5% Er_2O_3	1.09	
ZnO: 5% Er_2O_3: 1% Li_2O	1.05	2.70
ZnO: 5% Er_2O_3: 5% Li_2O	0.94	12.04
ZnO: 5% Er_2O_3: 10% Li_2O	0.83	21.19

horizontal furnace under constant N_2 flow at 950 °C for 10 h.

Secondary electron images were recorded either in a Leica 440 SEM or a FEI Inspect SEM. Cathodoluminescence (CL) spectra were recorded at room and liquid nitrogen temperature, in a Hitachi S2500 SEM operated at accelerating voltages between 15 and 20 keV. For recording spectra in the visible range, a HAMAMATSU PMA-11 charge coupled device camera has been used. In the infrared region, the detection system consists of a nitrogen cooled R5509 HAMAMATSU Photomultiplier tube and an Oriel monochromator equipped with a diffraction grating of 600 lines per mm and a blaze in 900 nm. X- Ray microanalysis (EDS) was performed with a Bruker AXS Quantax system in a Leica 440 SEM. μ-Photoluminescence (μ-PL) and Raman experiments were performed at room temperature in a Horiba Jovin Yvon LabRAM HR800 confocal microscope. A He-Cd laser ($\lambda_{ex} = 325$ nm) was used as excitation source for PL while, to avoid the resonance conditions, Raman spectra were recorded under excitation at 632.8 nm line of a He-Ne laser. For μ-PL, a custom designed module allows to separate excitation and collection point [17].

3. Results and discussion

After thermal treatments, a large amount of micro- and nanostructures are observed both on the alumina boat and on the tube walls. The morphology of these structures varies from sample to sample depending on the Li_2O proportion in the initial mixture. Fig. 1 shows the micro- and nanostructures obtained from the samples with single Er doping. Rods and needles of some tens of μm in length and diameters of hundreds of nm with hexagonal cross section are observed. As expected [18], the density and morphology uniformity of the samples grown from ZnS are higher than those obtained when ZnO is used as precursor. Moreover, the morphologies obtained are much simpler than the hierarchical structures obtained when ZnO is the starting point. Also, the temperature required when ZnS is used is about 250 °C lower than when using ZnO [18].

As have been already mentioned, the introduction of Li_2O changes dramatically the morphology of the structures obtained, even for the lowest Li content. In the case of samples with 1 wt% of Li_2O, besides the hexagonal rods observed in Er doped samples, long micro- and nanobelts are also observed (Fig. 2a). These structures are hundreds of microns in length and hundreds of nm width. When 5 wt% of Li_2O is added to the initial mixture, some screw shaped microstructures can also be observed (Fig. 2b). Finally, in samples with 10 wt% of Li_2O, nanobelts of lengths between hundreds of microns and tens of millimeters are mainly observed (Fig. 2c). The aspect ratio of these nanostructures is very high since their widths and thicknesses are typically in the range of 10 μm and 100 nm respectively (Fig. 2d). The change in the morphology associated to different dopants has been extensively studied. In particular, it has been previously reported that during the vapor-solid (V-S) growth the presence of different dopant species in the precursors lead to notable changes in the morphology in ZnO based systems. For instance, doping of ZnO with Mn [19], Mg [20], or Sn [21] give rise to hierarchical structures such as stacks of nanoplates, while Al incorporation leads to formation of nanoblades and microboxes [22]. The changes of surface energy due to dopant incorporation or local inhomogeneity of dopant distribution could be responsible of these modifications. Additionally, the facility of Li to diffuse could be also behind the changes observed. Similar variations have been also observed in Li doped Ga_2O_3 microstructures grown by the same method [23].

In order to study the crystal quality of the obtained samples, micro-Raman spectra on individual structures have been performed in the confocal microscope. Fig. 3 shows representative spectra recorded on microstructures of different compositions (5 wt% Er_2O_3 doped (red line), and 5% wt. Er_2O_3 − 5% wt. Li_2O codoped (green line)) samples, the spectrum of pure ZnO is also shown for comparison (black line). Peaks centered at 100 and 437 cm^{-1} (E_2 modes), 382 cm^{-1} (A1 TO mode), 413 cm^{-1} (E_1 TO mode) and multiphonon modes (205, 332 cm^{-1}), which are normally observed in the wurtzite ZnO are present [24,25]. However small shifts to lower frequencies in the spectra recorded on the microstructures containing Er are also detected. This shift is more pronounced in the 382 cm^{-1} (A1 TO mode) which is located at 375 and 373 cm^{-1} in the Er-Li codoped and Er doped microstructures, respectively. This behavior seems to be related to the incorporation of Er atoms into the ZnO matrix and has been previously observed in ZnO:Er and ZnO: Er, Li nanocrystallites [26].

The incorporation of Er as dopant in the grown micro- and nanostructures has been also investigated by EDX measurements. EDX mappings show that the incorporation is rather homogeneous along the structures, neither the morphology nor the Li content in the initial mixture seem to be relevant in the final Er distribution. This behavior also differs from Er doped ZnO nanostructures grown using ZnO as

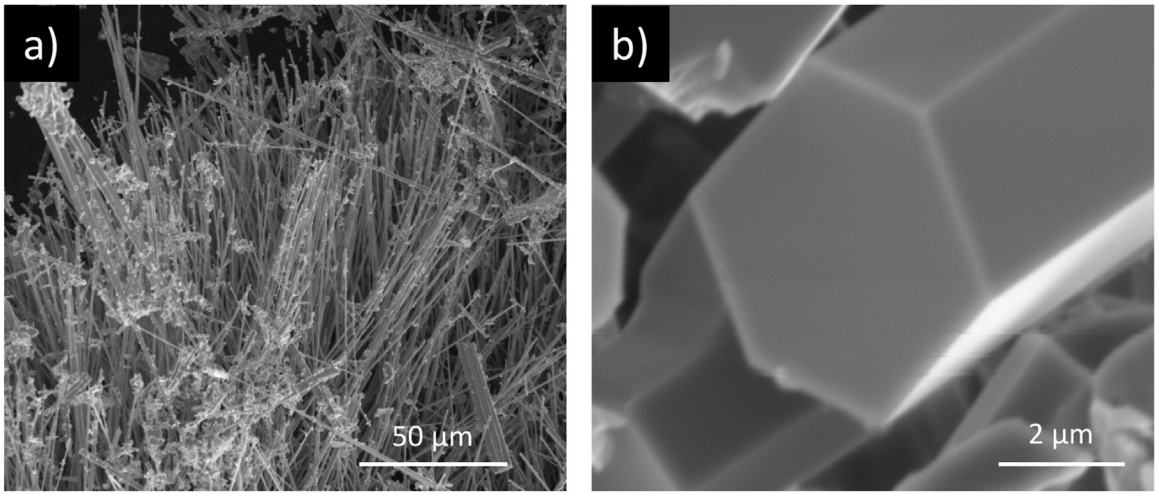

Fig. 1. SE images of a) structures grown in samples with single Er doping b) detail of the hexagonal cross section of a microrod.